COMPDYN 2011
ECCOMAS Thematic Conference on
Computational Methods in Structural Dynamics and Earthquake Engineering
M. Papadrakakis, M. Fragiadakis, V. Plevris (eds.)
Corfu, Greece, 25-28 May 2011

APPLICATION OF PDS-FEM TO SEISMIC FAILURE ANALYSIS OF REINFORCED CONCRETE BRIDGE PIER

M. Hori[1], K. Oguni[2], Y. Takahashi[3], T. Maki[4], S. Okazawa[5] and T. Yamashita[6]

[1]1Earthquake Research Institute, University of Tokyo,
Yayoi 1-1-1 Bunkyo, Tokyo, 113-0032, JAPAN,
hori@eri.u-tokyo.ac.jp.
[2]Department of System Design Engineering, Keio University,
3-14-1 Hiyoshi, Kohoku, Yokohama, Kanagawa, 223-8522, JAPAN,
oguni@sd.keio.ac.jp.
[3]Disaster Prevention Research Institute, Kyoto University,
Gokasho, Uji, Kyoto, 611-0011, JAPAN,
yos@catfish.dpri.kyoto-u.ac.jp.
[4]Division of Environmental Science and Infrastructure Engineering, Saitama University,
255 Shimo-Okubo, Sakura, Saitama, 338-8570, JAPAN,
maki@mail.saitama-u.ac.jp.
[5]Department of Transportation and Environmental Systems, Hiroshima University,
1-4-1 Kagamiyama, Higashi-Hiroshima, Hiroshima, 739-8527, JAPAN,
okazawa@hiroshima-u.ac.jp

[6]National Research Institute for Earth Science and Disaster Prevention,
1501-21 Nishikameya, Mitsuda, Shijimi, Miki, Hyogo, 673-0515, JAPAN,
tyamashi@bosai.go.jp.

Keywords: PDS-FEM, crack, concrete, seismic structure analysis

Abstract. *Particle-Discretization-Scheme (PDS) is a new discretization scheme which uses a pair of basis functions that discretize a function and its derivatives using characteristic functions, and PDS-FEM is an FEM which is implemented with PDS. It is straight forward to numerically solve a crack problem by means of PDS-FEM. This paper presents an application example of PDS-FEM to seismic structure response analysis of an RC bridge pier. A sophisticated non-linear elasto-plastic constitutive relation is used for concrete, and a detailed model is made. It is shown that the processes in which the pier is damaged and partially failed due to seismic loading are computed. Large plastic deformation as well as initiation and growth of local cracks in concrete are computed.*

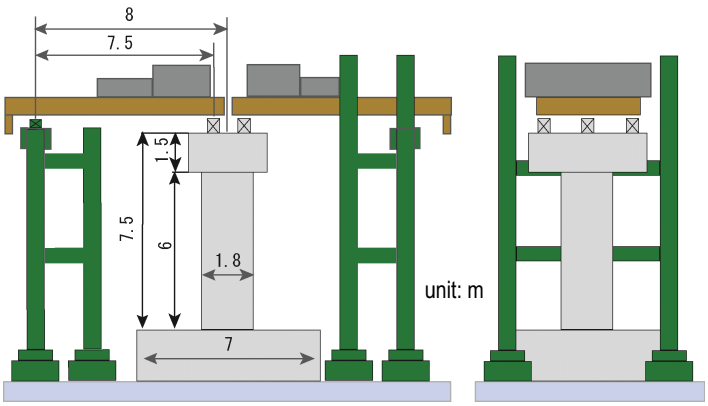

Figure 1: Schematic view of C1-1 Reinforced Concrete Bridge Pier.

1 INTRODUCTION

Earth Defense (E-Defense)[1] is the world largest shaking table that is capable to shake a full scale four story building. A project of Earthquake Simulator (E-Simulator) is aimed at building a virtual shaking table which numerically computes seismic response of a structure which even E-Defense cannot shake[2]. A solid element finite element method is used in E-Defense, so that only material constitutive relations are implemented in it even though large scale numerical computation is inevitable. ADVC is used as a base finite element analysis method in E-Simulator.

Reinforced concrete pier is a core target of E-Defense as well as E-Simulator. As an example, C1-1 Reinforced Concrete Bridge Pier, which was shaken by E-Defense, is presented in Fig. 1; the height of the pier reaches 7.5 m. There are two major characteristics in concrete materials. The first is brittle failure that is induced by single or multiple cracking. Closure of cracking or contact of crack surfaces is important as well as initiation and propagation of cracks.The second is constitutive relations (CCR), which expresses transition from elastic state to elasto-plastic state that accompanies material damage.

The implementation of cracking treatment and a sophisticated CCR into E-Simulator is thus needed. Cracking treatment of E-Simulator is made by applying a new discretization scheme, called Particle Discretization Scheme (PDS). PDS is implemented in E-Simulator. The most complicated but most reliable CCR is being implemented.

This paper briefly reports the current state of implementing PDS and CCR into E-Simulator. Concise but rigorous formulation for PDS and CCR is presented in Section 2. An example problem of seismic structure analysis of a concrete pier is solved in Section 3. This problem uses an E-Defense experiment of a real scale reinforced concrete pier.

2 FORMULATION

2.1 PDS

The main idea of PDS is the use of a characteristic function as a basis function of discretization[3, 4]. Let us denote by D and $\{\Phi^\alpha\}$ the analysis domain and a set of sub-domains of D, repsectively (D is decomposed into $\{\Phi^\alpha\}$). A basis function is ϕ^α, a characteristic function of Φ^α. A discretized function is thus expressed in terms of sub-domain-wise constant functions. This function has discontinuities across $\partial\Phi^\alpha$'s. Derivative of a function is computed by using a different domain decomposition of D. Denoting this decomposition by $\{\Psi^\beta\}$, the derivative is expressed in terms of ψ^β, which is a characteristic function of Ψ^β.

The implementation of PDS to FEM is straightforward. For simplicity, we consider the case that D is a linearly elastic body, and define the following functional for displacement, strain and stress ($\mathbf{u}$, $\boldsymbol{\epsilon}$ and $\boldsymbol{\sigma}$) is used:

$$J(\mathbf{u}, \boldsymbol{\epsilon}, \boldsymbol{\sigma}) = \int_D \frac{1}{2}\rho\dot{\mathbf{u}}\cdot\dot{\mathbf{u}} - \frac{1}{2}\boldsymbol{\epsilon}:\mathbf{c}:\boldsymbol{\epsilon} + \boldsymbol{\sigma}:(\boldsymbol{\epsilon} - \boldsymbol{\nabla}\mathbf{u})\,\mathrm{d}v, \tag{1}$$

where $\mathbf{c}$ and ρ are elasticity and density, $\boldsymbol{\nabla}\mathbf{u}$ is the gradient of $\mathbf{u}$, and $\cdot$ and : stand for the first- and second-order constraction. The variation of this J leads to the wave eqution,

$$\rho\ddot{\mathbf{u}} - \boldsymbol{\nabla}\cdot(\mathbf{c}:(\boldsymbol{\nabla}\mathbf{u})) = 0. \tag{2}$$

Discretizing $\mathbf{u}$ in terms of $\{\phi^\alpha\}$ and discretizing $\boldsymbol{\epsilon}$ and $\boldsymbol{\sigma}$ in terms of $\{\psi^\beta\}$, we now compute variation for the discretization coefficients and obtain

$$[M][\ddot{u}] + [K][u] = [f] \tag{3}$$

where $[u]$ is a vector for the coefficient of ϕ^α for discretized $\mathbf{u}$ and $[f]$ is a vector of the corresponding nodal force; $[M]$ is a diagonal mass matrix and its diagonal term is $\rho\Phi^\alpha$ with Φ^α standing for the volume of the sub-domain Φ^α; and $[K]$ is

$$k_{ij}^{\alpha\alpha'} = \sum_\beta c_{ipjq}\, b_p^{\beta\alpha}\, b_q^{\beta\alpha'} \tag{4}$$

with $b_p^{\beta\alpha} = \int_D \psi^\beta(\boldsymbol{\nabla}\phi^\alpha)_p\,\mathrm{d}v$.

When a traction-free crack is initiated or propagated onto a facet of $\partial\Phi^\alpha$, the constribution of $\boldsymbol{\nabla}\phi^\alpha$ in the integral of $b_p^{\beta\alpha}$ which is used in Eq. (4) is dropped. Additional boundary tractions need to be discribed on the facet, so that the traction free boundary conditions are met. As an approximation, the traction that has acted befor cracking is cancelled. In this manner, the reduction of $[K]$ and the change in $[f]$ due to the crack initiation or propagation can be rigorously computed in PDS-FEM.

2.2 CCR

Maekawa and his group[5, 6, 7] have proposed the most sophisticated and reliable CCR, which has the following two key relations:

$$\boldsymbol{\sigma} = \mathbf{c}:\boldsymbol{\epsilon}^E, \quad \mathrm{d}\boldsymbol{\epsilon}^P = \boldsymbol{\ell}:\mathrm{d}\boldsymbol{\epsilon}^E, \tag{5}$$

where d stands for the increment, superspcrit E or P designates elastic or plastic parts, respectively; $\mathbf{c}$ and $\boldsymbol{\ell}$ are functions of $\boldsymbol{\epsilon}^E$ which have been determined as experimental relations. An elasto-plasticity or instantaneous modulus tensor which gives strain increment-stress increment relation is thus given as

$$\mathbf{c}^{EP} = (\mathbf{c} + (\boldsymbol{\nabla}\mathbf{c}):\boldsymbol{\epsilon}^E):(\mathbf{I} + \boldsymbol{\ell})^{-1}. \tag{6}$$

where $\boldsymbol{\nabla}\mathbf{c}$ is a six-order tensor which gives the derivative of $\mathbf{c}$ with respect to $\boldsymbol{\epsilon}^E$ and $\mathbf{I}$ is the fourth-oder symmetric unit tensor.

As is seen, $\mathbf{c}^{EP}$ is not symmetric. Furthermore, it loses the positive-definiteness as $\boldsymbol{\epsilon}^E$ increases. The loss of the positive-definiteness will be a bottle neck for a solver which uses a conjugate gradient (CG) method or its extension. Beside the loss of symmetry and positive-definiteness, the numerical computation of $\mathbf{c}^{EP}$ is not trivial since it involves the computation of derivatives and an inverse tensor.

Table 1: Material properties used in numerical simulation.

a) concrete

Young's modulus	25,200 MPa
Poisson's ratio	0.2
compression strength	29.4 MPa
density	2,300 kg/m^3
critical strain for tensile failure	0.001339

b) steel

Young's modulus	197,100 MPa
Poisson's ratio	0.3
density	7,930 kg/m^3

The authors are proposing reformulation of Maekawa's CCR, assuming that an experimental relation between plastic and elastic invariants is a yield function, i.e., $J_2^P - H(J_2^E) = 0$, with H being an experimentally determined function and J_2 being the second invariant of the deviatoric part; this function yields a consistency condition that fully determines plastic strain increment. Indeed, when $\mathrm{d}\boldsymbol{\epsilon}^P = \mathrm{d}g\,\mathbf{d}$ is assumed with $\mathbf{d}$ being a second-order tensor which is experimentally determined, the increment of this yield function produces $\mathrm{d}g\frac{\mathbf{e}^P\mathbf{d}}{2J_2^P} = H'\frac{\mathbf{e}^E\mathrm{d}\mathbf{e}^E}{2J_2^E}$. Thus, the reformulated elasto-plasticity tensor is

$$\mathbf{c}^{EP} = (\mathbf{c} + (\boldsymbol{\nabla}\mathbf{c}) : \boldsymbol{\epsilon}^E) : (\mathbf{I} - \mathbf{L}). \tag{7}$$

where $\mathbf{L} = \left(DP\,\boldsymbol{\delta} + \frac{\mathbf{e}^E}{J_2^E}\right) \otimes \left((\frac{\mathbf{e}^E\mathbf{e}^P}{H'\,J_2^P} + 2)^{-1}\mathbf{e}^E\right)$.

Unlike the original equation, Eq. (6), $\mathbf{c}^{EP}$ of Eq. (7) does not involve computation of the inversion. Explicit expression of $\boldsymbol{\nabla}\mathbf{c}$ is obtained to further reduce numerical computation. Finally, the stress increment-strain increment is rewritten as

$$\mathrm{d}\boldsymbol{\sigma} = \mathbf{c} : \boldsymbol{\epsilon} + \mathrm{d}\boldsymbol{\sigma}^*, \tag{8}$$

where

$$\mathrm{d}\boldsymbol{\sigma}^* = -\mathbf{c} : \mathrm{d}\boldsymbol{\epsilon}^P + (\boldsymbol{\nabla}\mathbf{c} : \boldsymbol{\epsilon}^E) : \mathrm{d}\boldsymbol{\epsilon}^E. \tag{9}$$

Since $\mathbf{c}$ always satisfies the symmetryc and the positive-definiteness, a solver based on the CG method is applicable.

3 NUMERICAL SIMULATION RESULTS

As an illustrative example of PDS-FEM implemented with Maekawa's CCR, we compute the seismic response of the C1-1 which is shown in the introduction; see Fig. 1. The material properties of concrete and steel are summarized in Table 1. Linear tetrahedron elements are used, and the element number, the node number and the degree-of-freedom are 29,740,000, 4,860,000 and 14,580,000, respectively. Concrete and rebars are separately discretized; see Fig. 2. The input strong ground motion is presented in Fig. 3.

A super-computer SGI Altix 4700 Intel Itanium 1.66 GHz, 1 node $\times$ 256 core, is used for the computation. It takes 300 s for the computation of linear response at one increment of 0.01 s. The CPU time increases when plastic deformation becomes large as well as cracking takes place in the element. Cracking or the reduction of the element stiffness matrix is made according to the strength of material criterion; if the principal value of the element stress reaches the critical value of the strength, cracking takes place on a facet that is close to the principal value. It should be emphasized that the value of the reduced components of the element that suffers cracking is rigorously computed by using Eq. (4).

First, we examine the quality of the model. Eigen-values and eigen-vectors of the linear elastic deformation is computed, and the eigen-values are converted to the natural frequencies.

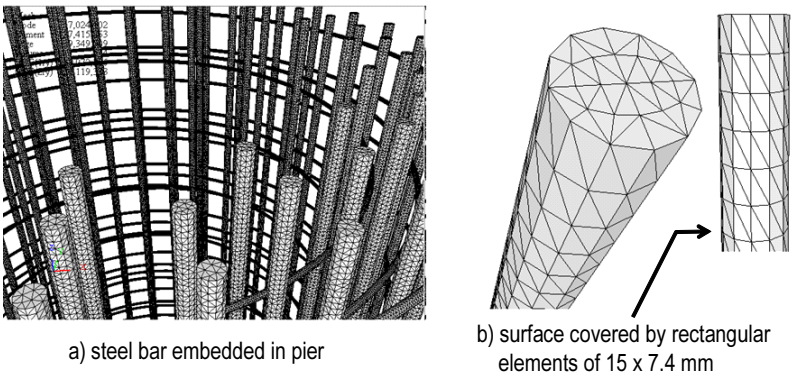

Figure 2: Examples of meshes used in analysis model.

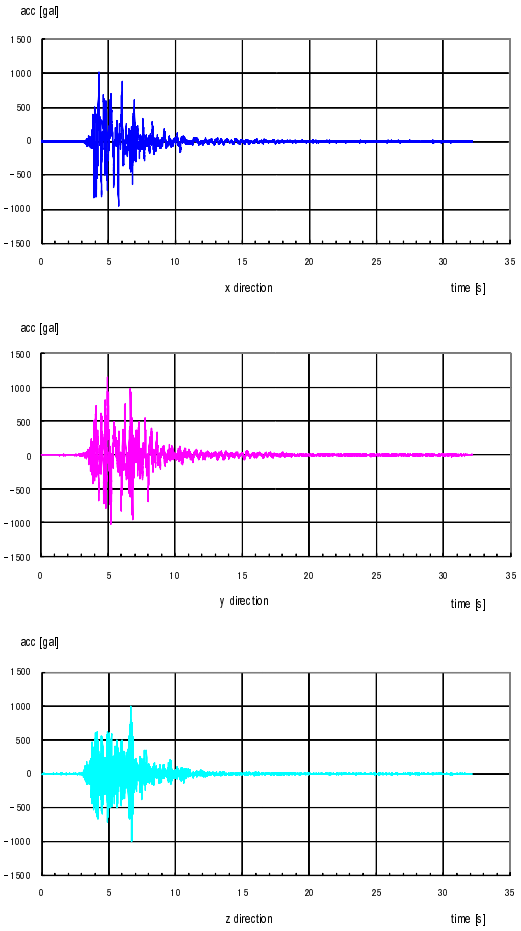

Figure 3: Input strong ground motion; time series of acceleration.

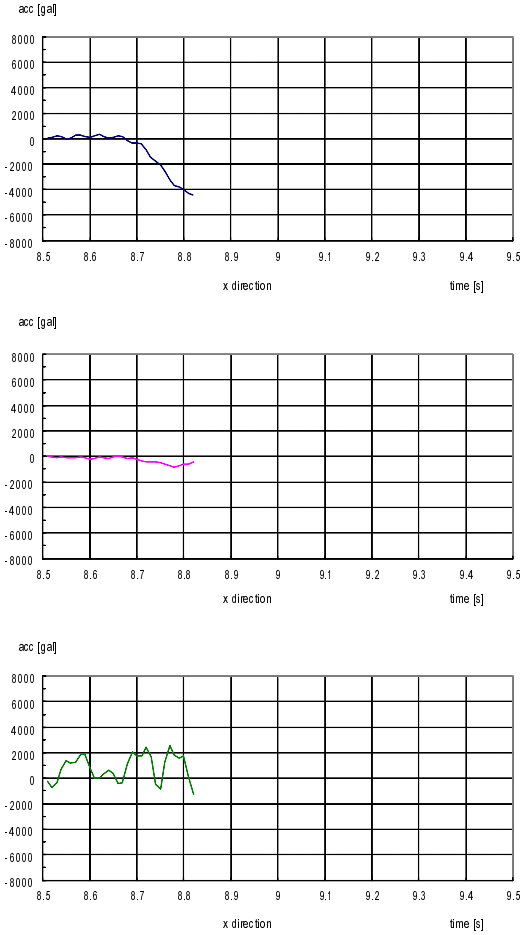

Figure 4: Seismic structure response computed for analysis model.

Table 2: First five natural frequencies of analysis model.

	frequency Hz	mode
1	2.58	1st bending normal to bridge axis
2	2.62	1st bending parallel to bridge axis
3	9.08	torsion
4	24.1	2nd bending normal to bridge axis
5	29.4	2nd bending parallel to bridge axis

Table 3: Number of broken element.

	number of broken elements		CPU time for 0.01 [s]	
time [s]	30 facets	60 facets	30 facets	60 facets
0.800000	0	0	360	420
0.810000	0	0	420	420
0.820000	0	0	420	360
0.830000	0	0	360	360
0.840000	0	0	420	480
0.850000	124	124	1200	1140
0.860000	1,778	2,055	8640	5340
0.870000	4,255	4,366	17400	9420
0.881914	7,094	7,170	24780	15600
0.891914	7,118	7,071	23340	13020
0.901914	21,867	22,654	67800	38640
0.911914	20,273	20,181	72180	38100
total	62,509	63,621		

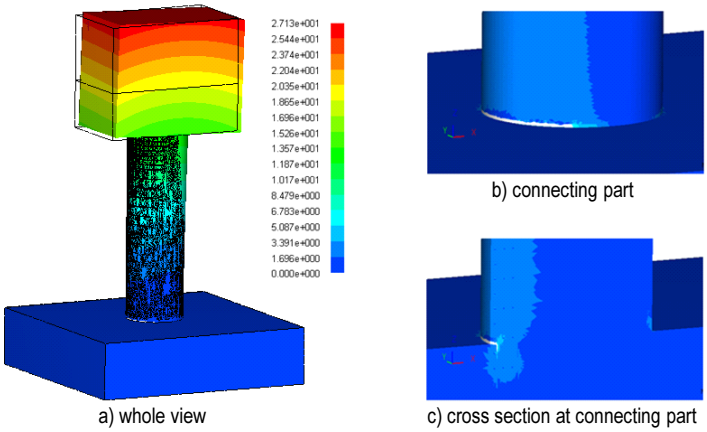

Figure 5: Schematic view of cracking at t =8.81 s.

The first five natural frequencies are shown in Table 2. These values are slightly larger than the experimentally measured data of the natural frequencies of the C1-1. The mode that corresponds to the natufral frequency is described in the table.

At this moment, the numerical computation is finished up to the input of first large shaking. The response of the top part of the pier is shown in Fig. 4. This response will be compared with the experimental data of E-Defense.

In PDS-FEM, cracking is made element-wise. The stiffness element and the nodal force increment are changed when one facet of an element is broken. Thus, it could take an unacceptable CPU time if non-linear computation is made every time one facet is broken, in order to carry out the most accurate computation. In this paper, we use the simultaneous cracking by specifying the maximum number of the facets of elements that are broken during one increment (0.01 s). The results of the number of broken element are summarized in Table 3, where the maximum number of the facets which are broken simultaneously is set as 30 or 60. As is seen, the number of the broken element does not differe significantly for the two cases. From now on, we set the maximum number as 60.

A schematic view of cracking is presented in Fig. 5; a) is the whole view of the pier and b) and c) are the closed-up view of the connecting part. The spatial distribuiton of the vertical normal

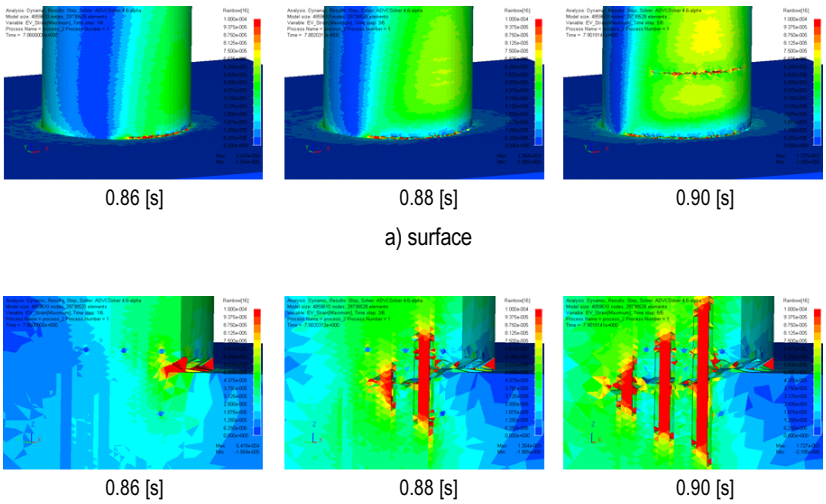

Figure 6: Distribution of broken elements.

stress component is shown. On the surface of the pier, cracking takes place at the connecting part (Fig. 5b)). The crack penetrates inside the pier (Fig. 5c)). The time series of cracking is presented in Fig. 6; a) is for the broken elements on the surface that have cracking and, and b) is for the broken elements inside the pier. The spatial distribution of the vertical normal stress component is plotted, to show that the stress is carried by steel rebars when cracking takes place in concrete.

We first have to admit that the results presented here are tentative and that a systematic evaluation will be made when the numerical computation is finished. At this momenet, however, it is shown that PDS-FEM is capable to simulate *multiple* cracking. In concrete, the crack tip is not broken uniformly, and a few parts of the crack tip are broken. By choosing suitable facets, PDS-FEM computes this cracking. Branching of cracks frequently occurs in concrete, and this cracking is computed, as well. It is certainly true that a model with the same configuration but different meshinng will produce different processes of cracking since PDS-FEM sues mesh boundary (or $\{\partial\Phi^\alpha\}$) as candidates of crack facets. A Monte-Carlo simulation of evaluating cracking processes or crack paths will be made by using a few models of the C1-1.

4 CONCLUDING REMARKS

This paper presents an application example of PDS-FEM to the seismic structure response analysis of the C1-1 that was shaken by E-Defense. A sophisticated CCR is implemented into ADVC, and detailed model is constructed. While the numerical computation is not finished, multiple cracking that is often observed in concrete is reproduced.

A sysmatic comparsion of the numerical results of PDS-FEM with the experimental data will be made, in order to clarify the limitations of PDS-FEM and to improve the treatment of cracking. A Monte-Carlo simulation of using different meshing will be made, as well, in oder to evaluate the variability of failure processes.

REFERENCES

[1] E-Defense, Hyogo Earthquake Engineering Research Center (E-Defense), National Research Institute of Earth Science and Disaster Prevention (NIED), Japan, http://www.bosai.go.jp/hyogo/ehyogo/index.html, as of 28 October 2009.

[2] Ohsaki, M., Miyamura, T., Kohiyama, M., Hori, M., Noguchi, H. Akiba, H., Kajiwara, K. and Ine, T.: High-precision finite element analysis of elastoplastic dynamic responses of super-highrise steel frames, *Earthquake Engineering & Structural Dynamics*, 38, 635–654, 2009.

[3] Hori, M., Oguni, K. and Sakaguchi, H.: Proposal of FEM implemented with particle discretization for analysis of failure phenomena, *Journal of the Mechanics and Physics of solids,*, Vol. 53(3), pp. 681–703, 2005.

[4] Wijerathne, M.L.L., Oguni, K. and Hori, M.: Numerical analysis of growing crack problems using particle discretization scheme, *International Journal for Numerical Methods In Engineering*, DOI: 10.1002/nme, 2009.

[5] Maekawa, K. and Okamura, H.: *Nonlinear Analysis and Constitutive Models of Reinforced Concrete*, Giho-Do, 1991.

[6] Maekawa, K., Okamura, H. and Pimanmas, A.: *Non-Linear Mechanics of Reinforced Concrete*, Taylor & Francis, 2003.

[7] Maekawa, K., Ishida, T. and Kishi, T.: *Multi-Scale Modeling of Structural Concrete*, Taylor & Francis, 2008.